S. CHAPULIOT, C. GOURDIN, J.P. MAGNAUD, CEA (France)
F. MERMAZ, IRSN (France)
A. MONAVON, Université Pierre et Marie Curie (France)

Hydro-thermal-mechanical analysis of thermal fatigue in a mixing tee

S. Chapuliot(1), C. Gourdin(1), F. Mermaz(2), J.P. Magnaud(3) and A. Monavon(4)
(1) DEN/DM2S/SEMT/LISN, CEA Saclay, F-91191 Gif Sur Yvette Cedex, France
(2) IRSN/DSR/SAMS, BP 17 F-92262 Fontenay aux Roses cedex, France
(3) DEN/DM2S/SFME/LTMF, CEA Saclay, F-91191 Gif Sur Yvette Cedex, France
(4) Université Pierre et Marie Curie, 4 Place Jussieu 75005 Paris, France

ABSTRACT
This article describes an approach developed by the CEA/DM2S to establish natural mechanisms (turbulence, pulsing and instability) which might be the cause of any substantial thermo-mechanical loading in a mixing area. This work is supported by IRSN and its main goal is to analyse, by calculation, the thermal loading caused by turbulent mixing in tees and to understand the mechanism of initiation and propagation of cracks in such components.

This study covers the thermo hydraulics and thermo mechanics fields and is carried out on the complex 3D geometry problem of the Civaux unit 1 case (which includes a mixing tee, elbows and straight sections) with the objective to understand the particularity of this configuration in which cracking occurred in a short time. Main question is: why through wall cracking appeared in such a short time?
All the study was made with the CAST3M code developed by the CEA.

Keywords: thermal fatigue, finite element method, thermal stress, temperatures loading, cracks propagation.

1. INTRODUCTION

The problem of fatigue in mixing areas, which is the subject of this article, occurs in pipes where flows at different temperature mix. If the rates of circulation of the fluids are high, the mixing is turbulent and results in temperature fluctuations that can be local or overall, depending on the form of the flow. When such thermal fluctuations are transmitted to the wall of the structure, a mixing tee or a simple branch, the strain variations result in fatigue damage and cracking.
The problem is complex and involves four scientific disciplines which have their own difficulties and scientific limitations:

- thermal-hydraulic field, as concerns the thermal loading (turbulent mixing of two fluids),
- thermal field, as concerns the initial interface of the problem, as a result of heat exchange between the fluid and the wall,
- mechanical field, as concerns the response of the structure to the complex thermal challenge to the inner surface,
- the science of materials, as concerns the strength of the materials making up the structure subjected to the challenge.

The various difficulties associated with theory, experimenting and modelling result in the fatigue problems of the mixing areas observed in the facilities are not being well understood:

- The appearance of a network of cracks is known but not properly controlled. The phenomenon of thermal stripping has long been known and analysed, particularly for the fast breeder reactor structures vulnerable to this type of damage [1]. It is still not fully understood how to determine the conditions of initiation of elephant skin crack from a temperature load (temperature difference between two fluids) as concerns location, position, and variation over time.
- Propagation through the wall of macro-cracks resulting from the thermal stripping and the presence of discontinuities (discontinuities of geometry and/or material, such as a weld), is far rarer (in most cases, the cracks remain at the surface) and this phenomenon is even less well understood. The problems encountered in a mixing tee in the residual heat removal system of the Civaux unit 1 [2] is an example of this type of damage that is not explained by the 1D analyses that cannot demonstrate through-wall penetration.

It is to clarify this point, particularly by research into loading that can result in through-wall cracks, that mechanical studies have been initiated to gain a fuller understanding of the problem. The goal of these studies is to supply the information that cannot be provided via 1D analysis by seeking to determine the overall response of the structure to the thermal challenge. These are of the 3D type, and are necessarily dependent on precision and knowledge of the thermal loading. As investigation of the thermal load imposed on the structure remains difficult, a special approach was developed, which is described in this article. Furthermore, this work was supported by IRSN.

1 THE APPROACH

The first stage of our approach consisted of a mathematical analysis of the thermal loading, followed by a mechanical analysis of the associated mechanical loading. This was based on experimental temperature readings with the most realistic smoothing possible between them. This thermal challenge obviously had little physical reality as it was a mathematical construct, but it offered the advantage of being rapidly setting up and independent of successful thermal-hydraulic calculation or link-up between the different computer codes. Furthermore, the parameters are more easily set, making it possible to more rapidly begin the study of the local and global responses of the structure.

The second stage essentially consisted of a complete Hydro-Thermo-Mechanical (HTM) numerical analysis carried out with the CAST3M computer code. This used the existing computing resources (LES simulation) and was thus subject to their limitations and uncertainties. The main advantage of this approach was that it provided an example of mixing fluctuations in a tee, enabling subsequent deduction of the mechanical response of the structure (spatial distribution, through the thickness, average stress, frequency response etc.). Although it may have been approximate, the solution offered the advantage of providing initial results for orientating the subsequent work. In addition, this approach made it possible to implement the entire calculation sequence, to identify the problem areas and to initiate study of the tools and requirements for the interfaces between the different computing resources (particularly between the thermal-hydraulic calculations and the thermal-mechanical calculations).

The third stage consisted in applying and using the knowledge acquired to a case encountered in the field. The incident that occurred in the residual heat removal system of the Civaux unit 1 constituted an excellent example of the phenomena associated with thermal fatigue.

2 DESCRIPTION OF THE CIVAUX 1 CASE

Following the discovery of a leak due to a longitudinal crack at the outer edge of elbow in a mixing zone of the Residual Heat Removal System of the Civaux NPP unit 1 in 1998,

metallurgical expertises were carried out and highlighted that the origin of this degradation phenomenon was due to cracking by thermal fatigue. The incident that occurred in this system was caused by thermal fatigue associated with fluctuations in the temperature of the fluid at the mixing tee. However, the mechanisms that caused the transition from crack initiation to the development of a set of cracks of a significant depth in a relatively short length of time, has not been precisely established

The overall system is shown in Figure 1. The section of interest is that beginning at Valve 101VP (hot leg) and Valve 071VP (cold leg) up to the tee and downstream of it (framed). The system is at a pressure of 36 bar. The hot leg contains water at 180°C with a flow rate of Q_c and the cold leg contains water at 20°C with a flow rate of Q_f. The total flow rate Q_f+Q_c is 550 m^3/h. The flow ratio $Q_f/(Q_f+Q_c)$, which was analysed, corresponds to 20%.

A number of analyses were made to understand how, under the effect of thermal fluctuation loading, cracks could appear and develop through the wall of an elbow in such a short length of time (1500 h). Metallurgical examination also revealed substantial cracks and networks of small thermal fatigue cracks in the vicinity of the welds, in the absence of fabrication defects. The damage was mainly located:

- on the outside of the elbow downstream of the mixing tee (a),
- in the mixing tee (b),
- at the bottoms of the weld beads and at the circumferential weld roots (c),
- in the straight sections of piping (after longer periods of operation) (d).

3 THERMAL-HYDRAULIC ANALYSIS

3.1 Description of the system

The first mesh (RRA2C, see Figure 2) was limited to the first two upstream elbows. The second mesh (RRA4C, see Figure 3) included the three elbows upstream of the hot leg between the tee and the valve as well as the elbow downstream of the cold leg. The effect of the valves on the flow was not taken into consideration.

3.2 Physical analysis

3.2.1 Flow regimes

The flow velocities (U_D) were 0.59 m/s and 2.97 m/s respectively in the cold leg and the outlet section (combining the two flows). The corresponding Reynolds numbers ranged from $1.5.10^5$ to $3.9.10^6$. The flow is unstabilised and turbulent in the two legs, with statistically stationary boundary conditions. The floatability effects could be assessed by calculating a Richardson number that varied between 0.9 and $2.6.10^{-2}$. The effects of natural convection were of minor importance without being negligible at the point of actual mixing in the tee. These were modelled using the Boussinesq approximation.

3.2.2 Timescales

Upstream of the tee (hot and cold legs), the straight tube lengths were not sufficiently long for a stable regime to be established (as they only corresponded to six diameters). The model of flow in a pipe could nevertheless be used to estimate the characteristics of the turbulence and the inlet of the tee.

Turnover time

The turn over time is the longest period that can be associated with a turbulent structure. It is of the order of $T_R = L/U_*$ where L is the characteristic size of the energetic turbulent structure in a duct and U_* is the friction velocity. L was taken to be equal to D, the largest size for a turbulent structure liable to pass through the duct. At the hot and cold flow intersection (in the

tee), an energy structure could be associated with a temperature variation of the order of the temperature difference between the two currents. In other words, it was considered that the two flows only mixed slightly at this level. The time scale associated with these turn over times characterized the persistence time of a temperature fluctuation due to turbulence.
To evaluate U_*, use was made of pressure losses correlations in a duct.

Transit time
At a given point, a set of turbulent structures pass along the wall at a velocity of U_D. The order of magnitude of the transit time of the largest turbulent structure is: $T_T = L/U_*$. The transit times are considerably shorter than the turn over times. The wall can thus experience the passage of turbulent structures as though they were still. This is a conventional approximation in the case of high-velocity flow.
The consequence is that **the wall could not be influenced by convected turbulent structures of characteristic time greater than the transit time;** it would only see a small proportion of it, as convection acts as "high-pass" filter. The lower frequencies that the wall was exposed to and originate from turbulent structures corresponded to the inverse of the transit times. Table 1 shows the estimates that could be made. The flow velocity distribution actually remained very heterogeneous in the outlet section (as will be seen). The frequencies associated with the transit times ranged from 2.5 to 12 Hz.

	Transit time	Frequency	Turn over time	Frequency
Outlet section U = 2.83 m/s	0.08 s	12.5 Hz	1.6 s	0.625 Hz
Cold leg U = 0.47 m/s	0.4 s	2.5 Hz	8 s	0.125 Hz

Table 1 – Characteristic times

An analysis in greater depth was detailed in [10].

3.3 Large-scale instability
Another source of thermal fluctuations may be caused by non-convected large-scale instability such as that associated with pulses, pump fluctuations, gravity waves etc. These instabilities must remain constant on average over time or evolve slowly:

$\int_0^T u'.d\tau \neq 0$ for T to be sufficiently long, whereas for a turbulent fluctuation: $\int_0^T u'.d\tau = 0$

In view of the preceding analysis, these were the only phenomena capable of generating sufficiently low frequencies.

3.4 Thermal-hydraulic modelling

3.4.1 Large-Eddy Simulation (LES)
The LES approach consists of filtering the Navier-Stokes equations at a scale with a length corresponding to the sign of a mesh element. The effect of sub-element fluctuation is modelled by adding a viscosity. The Smagorinsky model [5] is that most commonly used:

$$\mu_S = c_S h^2 \left| \nabla \tilde{U} + \nabla \tilde{U}^T \right|,$$

where $c_S = 0.01$ is the Smagorinsky constant, h is the size of the filter and $\tilde{U}$ was the computed velocity.
However, for the approach to be valid, it is necessary for all the scales corresponding to the energetic turbulent structures to be solved. The meshes which we used did not fully meet this requirement, and we therefore name our approach VLES.

3.4.2 Wall model

As in k-ε modelling, the conditions at the boundaries were given by the wall functions written on the edge of the mesh. As the difference between the edge of the mesh and the wall (0.1 mm) corresponded to the thickness of the logarithmic zone, these laws reflected the behaviour of turbulent structures that were sufficiently small for them not to be solved. It was therefore reasonable to accept that they retained their statistical values.

3.4.3 Inlet boundary conditions

The hot leg and cold leg temperatures were constant, and equal to 20 and 180°C respectively. For each component of the flow velocity, a random firing was made for all the inlet face points so that on average, the standard deviation and a correlation length were imposed. The fluctuation along the flow was set at 5% of the flow velocity and the cross-wise fluctuations were set at 2.5%. The correlation length was 0.2 R (where R was the radius of the duct).

$$u_i = \bar{u}_i + u_i' \quad \text{with: } \left\|u_i'\right\|_{//} = 0.05.\bar{u}_i \text{ and } \left\|u_i'\right\|_{\perp} = 0.025.\bar{u}_i$$

To introduce a time correlation (spatial in the direction of flow), two successive random firings were linked, separated by a correlation time $T_c = L_c/U_D$ where L_c was the previously defined correlation length. At a given time between the two firings (i and j), the disturbance (X) was a linear combination of the firings at instants i and j:

$$X(n\Delta t) = (1-\alpha).X_i + \alpha.X_j, \text{ where } \alpha = \frac{n\Delta t}{T_C}$$

The random nature of the disturbance was justified only by the need to avoid preferential excitation of certain frequencies and not as a result of its similarity with a turbulent fluctuation. This disturbance was used to initiate the development of a phenomenon which was governed (at least in the context of linear stability) by a problem of which the boundary conditions were homogeneous and which could not begin autonomously.

3.4.4 Heat at wall

All the ducts in the sections of interest were heat lagged. Loss of heat was considered to be negligible. This made it possible to decouple the thermal-hydraulic calculation from the thermo-mechanical calculation for the wall by imposing non-null flux at the wall.

3.4.5 Numerical method

The calculations were made with the CAST3M code. A non-conformal Q2–P1 quadratic finite element was used. The pressure was discontinuous. Opting for quadratic elements resulted in the approximation of the temperature gradients (in particular) being of the second order instead of the first order for linear elements. This gave substantially more accurate results. The algorithm used was an incremental projection algorithm [6] [7]. The time scheme was of the second order (BDF2 scheme).

3.5 Results of calculation and comments

3.5.1 RRA2C calculation (two upstream elbows)

The calculation was carried out over 20 seconds of physical time. Figure 4 gives the temperature averaged over the last 10 seconds. Two mixing zones were observed (orange to green) at the interfaces between the hot and cold flows. The first, at the tee, was semi-circular on the outer surface of the tee. The second, which was twisted, was located in the downstream section at the outlet of the elbow. The extent of the green zone gives a measure of the amplitude of the pulsing. At the tee, the amplitude remained very small.
The standard deviations of the temperature were calculated over the last 10 seconds. This was sufficient to obtain convergent statistics. The maximum standard deviation (see Figure 5)

were 74°C and located at the tee, on the same side as the upstream elbow and were very localised. The average standard deviation was 40°C in particular in the downstream section.

3.5.2 RRA4C calculation (four upstream elbows)

The hot leg valve is considerably further upstream than the elbow modelled in the RRA2C geometry. But the presence of a series of elbows and straight sections between the two could substantially change the velocity profiles. This led us to make the RRA4C calculation (see Figure 3). Here the geometry far more accurately replicated the residual heat removal system. Nevertheless, no disturbances associated with the presence of valves were modelled.
Figure 6 shows the standard deviation integrated over the last 2.5 seconds and confirms the observations made concerning the temperature histories. The zone of greatest fluctuation was still in the vicinity of the nozzle on the outer surface. However, this zone was considerably thicker than in the RRA2C case (see Figure 5). An initial explanation of this extremely high instability was provided by the iso-flow velocities of friction used to trace the flow in this isothermal section (see Figure 7). This plot showed the presence of twisting of the flow in the hot leg upstream of the tee. The excess flow on the outside of the elbow reappeared at the inner profile in a position that was virtually symmetrical.

3.6 Conclusions of the thermo hydraulic study

The physical analysis enabled us to clarify the role that turbulence can play in challenging the structure. Although it may have been the cause of the thermal stripping (high frequencies), it alone could not explain the crack propagation. The main reason was the way in which convection acted as a high-pass filter which prevented the wall from experiencing convected thermal fluctuations of frequencies greater than the inverse of the transit time (2.5 Hz in the outlet section). These frequencies were still too high to explain the large crack propagation.
The calculations that we made indicated that boundary condition excitation with white noise triggered pulsation of relatively great amplitude. The turbulence was therefore the probable natural origin of the low-frequency instability in the decay heat removal system.
However, the geometry of the upstream hot leg played a major role in either amplification or damping of the pulses. The RRA4C geometry, which was closest to the actual geometry (extending up to the valves), was the most destabilising. The sequence of three elbows and straight sections resulted in substantial twisting of the flow at the inlet of the tee.
The RRA2C geometry, limited to the upstream elbow at the hot leg inlet, actually substantially reduced the amplitude of the pulses at the tee.

4 LINKED-UP ANALYSIS OF THE RRA4C CALCULATION

The goal of the hydro-thermo-mechanical link-up made with the RRA4C geometry was analysis of the areas in which cracks appeared, particularly the outside of the outlet elbow for which no analysis could explain the crack propagation which created a major leak observed in the field.

4.1 Description of the linked-up analysis

Generation of the meshes of the structure was directly based on the meshes used for the thermal-hydraulic calculations, the thickness of the tee being 30 mm and the thickness of the elbow and the pipes being 9.3 mm. The transition zone between the tee and the elbow or the pipes was taken into account. The size of the first mesh in the tee was set at 0.75 mm, and the size of the mesh in the elbow and the pipes was set at 0.28 mm. This discretisation enabled us to obtain all the changes of the different variables at a frequency of 10 Hz.
The material and the line modelled were considered to be thermally and mechanically linear. Properties of the material were those of austenitic steel at room temperature.
Thermal properties:

- Linear conduction K = 14.7 W/m°C,

- Specific heat Cp = 480 J/kg/°C,
- Density ρ = 7800 kg/m^3.

Mechanical properties:

- Modulus of elasticity E = 177,000 MPa,
- Poisson's coefficient ν = 0.3,
- Coefficient of thermal expansion α = 16.10^{-6} /°C.

The thermal loads were derived from the RRA4C thermal-hydraulic calculations. The physical time modelled corresponded to a sequence of the last 10 seconds. The fluid temperature fields were used as input data for the thermo-mechanical calculations. The heat transfer between the fluid and the structure took place without approximation as the two meshes were created at the same time and the nodes on the inner surface of the structure coincided with those of the fluid model. The coefficient of heat exchange between the fluid and the inner wall was taken to be constant whatever the temperature (from 20°C to 180°C) and over time. Also, it was assumed that the structure was ideally heat lagged on the outside and that there was no exchange of heat with the exterior (null-flux condition).

The mechanical boundary conditions were set so that:

- Displacement of the cold section was prevented (lower elbow inlet). This section being the farthest from the mixing zone, its influence would be small.
- Rotation was prevented but not of displacement of the outlet and hot inlet sections.

Establishing these conditions was a delicate matter as it was difficult to determine the actual stiffness of the upstream and downstream lines.

4.2 Determination of the temperature fields in the structure

The thermal calculation was carried in five successive 10-second sequences to obtain a stabilised response for the structure. The temperature variation at the inner surface is shown in Figure 8. It can be seen that there is a broad zone with a high ΔT, of around 119°C. This value is substantial and represents 75% of the maximum ΔT (i.e. Tc-Tf). This zone extends from the outer surface to the inner side of the mixing tee opposite the hot inlet. This zone of extreme temperature variation encompasses the tee to elbow transition zone and corresponds to the oscillating motion of the cold front observed in the average calculations.
Furthermore, in a small region downstream of the mixing tee, at the intersection of the hot and cold pipes, there are substantial temperature variations, but at high frequency and extremely localised.
As concerns the outside of the elbow, temperature variations of around 50°C also occur, as well as significant temperature variations (ΔT > 50°C) in the outlet tube.

4.3 Determination of the stress fields in the structure

4.3.1 Average calculations

On the basis of the average temperature determined in the structure, the average thermal stresses were determined by a thermo-mechanical calculation. Figure 9 shows the equivalent stress distribution fields (in the Von Mises sense) at the inner surface. The maximum value of the equivalent Von Mises stress reached 358 MPa. The tee-to-elbow transition zone and the inside of the elbow were also places where these high stresses occurred. On the outside of the elbow, the average stress was very low.

4.3.2 Fluctuating calculations

An important stage of analysis of the mechanical state consisted in determining the value of the equivalent variation of the stress in the Von Mises sense at all points in the structure. An iterative procedure was used for obtaining the equivalent variation.

Determining the maximum variations of σ_{eq} involved calculation of the stress variation between two instants, then determination of the maximum for the entire loading sequence. Between the two instants t_i and t_j (or calculation steps i and j), the variation of the equivalent stress was determined as follows:

$$\Delta\sigma_{eq}^{ij} = \frac{1}{\sqrt{2}}.\sqrt{(\Delta\sigma_{xx}-\Delta\sigma_{yy})^2+(\Delta\sigma_{yy}-\Delta\sigma_{zz})^2+(\Delta\sigma_{zz}-\Delta\sigma_{xx})^2+6.(\Delta\sigma_{xy}^2+\Delta\sigma_{yz}^2+\Delta\sigma_{zx}^2)}, \text{ with:}$$

$$\Delta\sigma_{\alpha\beta} = \sigma_{\alpha\beta}{}^{i} - \sigma_{\alpha\beta}{}^{j} \quad (\alpha,\beta = x, y \text{ or } z)$$

The maximum value of all the possible pairs of calculation steps was therefore (for n calculated steps):

$$\Delta\sigma_{eq}^{MAX} = MAX\left[\Delta\sigma_{eq}^{i=1..n,\, j=i+1..n}\right]$$

Note: As the maxima did not appear at the same instants, the resulting field did not correspond to a state of equilibrium. Neither could it be used to determine the spatial averages (bending or membrane stress for instance).

Figure 10 shows the distribution of the variation of the equivalent stress in the Von Mises sense at the inner surface for the four-elbow configuration. The maximum value of the equivalent stress variation was 467 MPa. The area where the variation was the greatest was located in the tongue extending from the inside and extending up to the tee on the side opposite the hot fluid inlet. Other zones were distinguished where the equivalent stress variation was significant, particularly on the outside of the elbow with values of 180 to 225 MPa, as well as at the outlet of the straight section downstream of the mixing tee. It was noted that there were values close to 100 MPa on the inside of the elbow.

4.4 Study of the propagation

The material of which the elbow and the mixing tee were made is 304L steel, with a Paris law of the following form:

$$da/dN = C.(\Delta K_{eff})^n$$

C and n are material coefficients as defined in document RCC-MR [8] equating to $7.5.10^{-10}$ for C and 4 for n.

The effective stress intensity factor was determined by calculating ΔK_I and function q(R) such that:

$$\Delta K_{eff} = q(R).\Delta K_I, \text{ with } q(R) = \frac{1-0.5.R}{1-R} \text{ for R>0 then } q(R) = \frac{1}{1-0.5.R} \quad (R=K_{min}/K_{max})$$

Stress intensity factor K_I was determined by analysis of the stress profile through the thickness of the component. For each point treated, the stress profile in the thickness was derived for the duration of the sequence (10s). By identification, at each instant of calculation, the values of coefficients σ_0, σ_1, σ_2, σ_3, and σ_4, were determined by smoothing the stress profile through the thickness with a 4-degree polynomial. Then the influence coefficient values (i_0, i_1, i_2, i_3 and i_4) were used, being tabulated as a function of the structure and the defect [8], the stress intensity factor being expressed as follows:

$$K_I = \left[\sigma_0.i_0 + \sigma_1.i_1.\frac{a}{h} + \sigma_2.i_2.\left(\frac{a}{h}\right)^2 + \sigma_3.i_3.\left(\frac{a}{h}\right)^3 + \sigma_4.i_4.\left(\frac{a}{h}\right)^4\right].\sqrt{\pi.a}$$

Where *a* corresponds to the depth of the defect and h to the thickness of the component. ΔK_I could be determined by counting the cycles with the Rainflow method, for instance [9].

4.4.1 Application to the case with four elbows

The case of the outside of the elbow
On the basis of the circumferential stress, the stress intensity factor was determined (see Figure 11). Then, function q(R) was determined, depending on load ratio R. For each crack advance increment, the corresponding number of cycles was obtained, then, by integration, the number of cycles to progress from a crack of a/h = 0.1 to a/h = 0.8 (6.92 mm), i.e. 372,720. By considering the two major cycles per sequence of 10 seconds (see Figure 11), a propagation time of 517 hours was obtained..

The case of the tee-to-elbow transition: thick part of the thickness transition
The first point treated (a in Figure 10) was located in the thick part of the mixing tee. On the basis of the longitudinal stress profiles, the stress intensity factor over time was determined, for different crack depths. The type of defect treated was an internal circumferential defect. But, the intensity factor became negative from a crack depth of 6 mm (i.e. a/h of 0.2). The propagation then stopped (see Figure 13).

The case of the tee-to-elbow transition: thin part of the thickness transition
The second point treated (b in Figure 10) was located in the thin point of the mixing tee, in the close vicinity of the preceding point, in order to qualify a possible thickness effect. The two points were subjected to substantially equivalent surface stress. The type of defect treated was an internal circumferential defect. A number of cycles to reach a crack length of 6.92 mm (a/h = 0.8) was 21,388. The extremely rapid propagation of the crack can be explained by important stress intensity variation in this area (see Figure 12).

5 GENERAL CONCLUSIONS

This paper contains an analysis of the mixing tee of the Civaux unit 1. Metallurgical examinations of the residual heat removal system mixing tee revealed the presence of substantial cracks as well as local thermal fatigue cracks:

- in the mixing tee,
- on the outside of the elbow,
- in the straight sections of the line.

The cracks observed in the mixing tees and the connection with the piping were substantially explained by the various calculations made, as this area is shown to be strongly loaded and subjected to strong temperature fluctuations. In the case study described in this paper, the stress variation levels are in the region of 570 MPa (in a relatively small area) in the four-elbow configuration. Allowance made for the coarse description used for this area; these levels explain the appearance of cracks.

As concerns the thermal fatigue cracks downstream of the elbow in the straight section of the line, the calculations showed that they could be due to twisting of the velocity of the fluid flow in this duct. The case considered in this article showed that the variations of equivalent stress were of the order of 250 MPa in the four-elbow configuration. The location of these zones where the thermal fluctuation was substantial was more than two diameters downstream of the elbow, as observed in practice at Civaux unit 1.

The critical point of the Civaux unit 1 incident was the appearance of a crack on the outside of the elbow and its rapid propagation through the wall. Before this study, no load had been identified that could explain the cracking in this zone. The calculations described in this article show the importance, in understanding this phenomenon, of making allowance for a

substantial length of line with the various elbows upstream. The reference calculation (RRA2C) only included two elbows and no significant thermal or mechanical load was found. When allowance was made for a greater length of line upstream, with the various elbows present in it (RRA4C), evidence was found of large-scale instability of greater amplitude. This large-scale instability gave rise to pulses which were characterised by the presence of significant thermal fluctuations. It is to be noted that this instability was triggered by high-frequency random fluctuations. These were therefore equivalent to average flow oscillation "specific modes" triggered by turbulence.

In addition, on the basis of the analysis of the surface stress, a study of crack propagation in depth was made. It was then observed that, for the thin sections, the outside and the outlet of the tee, the calculated challenges resulted in very rapid propagation until the wall was breached. In particular, on the outside of the elbow, once a crack was initiated at the surface, it propagated through the wall in 500 hours. This result is important as it represents **evidence for a thermal load strong enough to cause a through-wall crack**. For the thick parts, the values of ΔK cancelled out, resulting in stopping of crack growth at 6 mm.
A most comprehensive and detailed article is available in the Nuclear Engineering and Design review [10].

6 ACKNOWLEDGEMENTS

The authors would like to thank the Cast3M team consisting of T. Charras, A. Millard and P. Verpeaux for the assistance they provided in setting up the coupled thermal-hydraulic calculations.

7 REFERENCES

[1] O. Gelineau, J.P. Simoneau, M. Sperandion et J. Guinovart, "*Review of predictive methods applied to thermal stripping problems and recommendations*", Proc. SMIRT 15, Paper F06/3, Seoul, 1999.
[2] C. Faidy *et al.* "*Thermal fatigue in French RNR systems*", In Int. Conf. on Fatigue of Reactor Components, Vapa, California, 2000.
[3] H. Schlichting, "*Boundary-layers Theory*", McGraw-Hill book company, 1968.
[4] B.E. Launder, "*In Turbulence models and their applications*", Eyrolles : Ecole d'été d'analyse numérique CEA-EDF-INRIA 56, 1984.
[5] J. Smagorinsky, "*General circulation experiments with the primitive equations*", Mon. Weath. Rev. 91, 3:99-164, 1963.
[6] J.L. Guermond, "*Sur l'approximation des équations de Navier-Stokes par une méthode de projection*", C.R. Acad. Sci. Paris, 319:887-892, 1994.
[7] A. Ern and J.L. Guermond, "*Eléments finis : théorie, application, mise en œuvre*", Springer : Mathématiques et Applications 36, 2001.
[8] B. Drubay *et al.*, "*A16 : Guide pour l'analyse de la nocivité des défauts et Fuite Avant Rupture*", RCC-MR, 2002.
[9] "*Fatigue sous sollicitations d'amplitude variable, Méthode Rainflow de comptage de cycles*", Norme AFNOR, A3-406, 1996.
[10] S. Chapuliot, C. Gourdin, T. Payen, J.P. Magnaud and A. Monavon, "*Hydro-thermal-mechanical analysis of Thermal Fatigue in a Mixing Tee*", Nucl. Eng. and Deign 235 (2005) 575-596

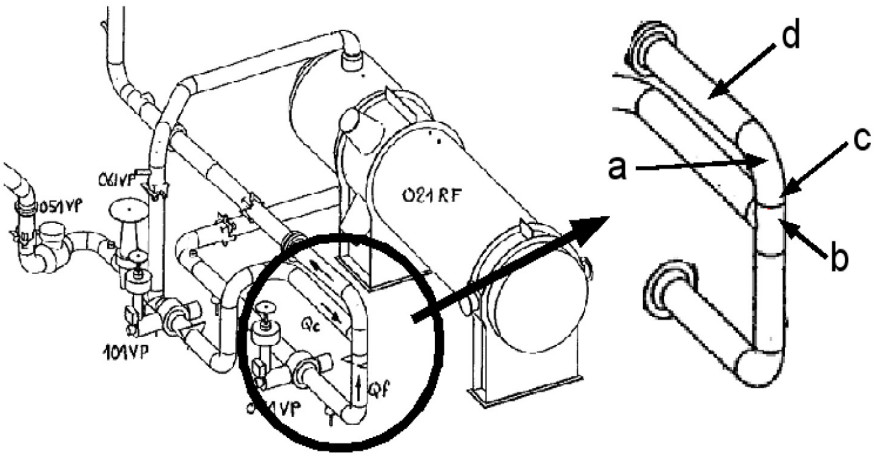

Figure 1: Overall view of the loop

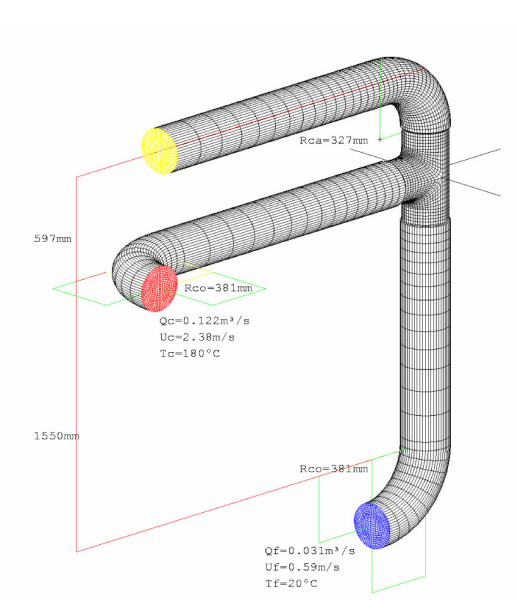

Figure 2: Mesh of system (RRA2C)

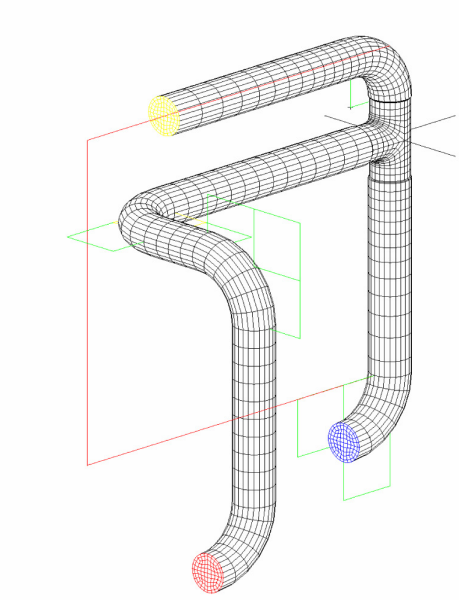

Figure 3: Mesh of system (RRA4C)

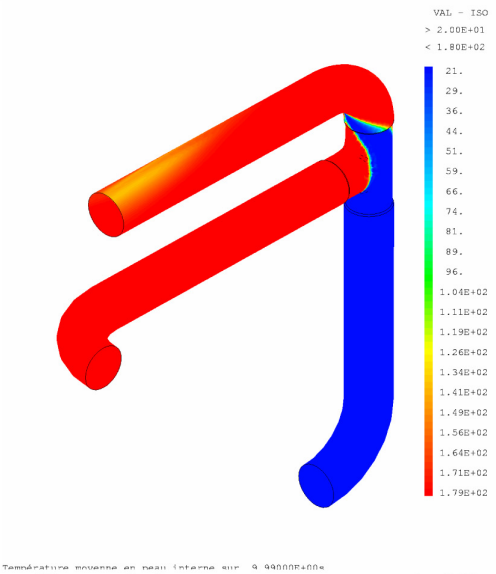

Figure 4: Average temperatures in °C

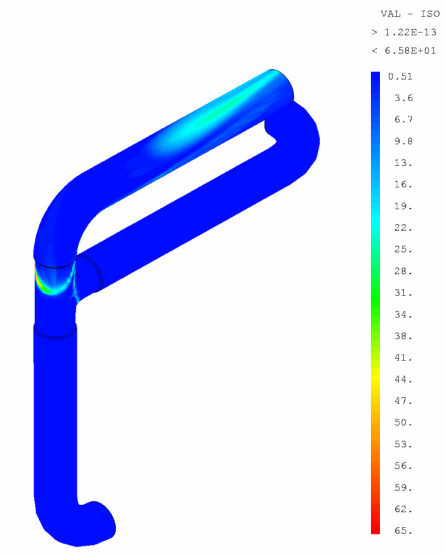

Figure 5: Standard deviations in °C

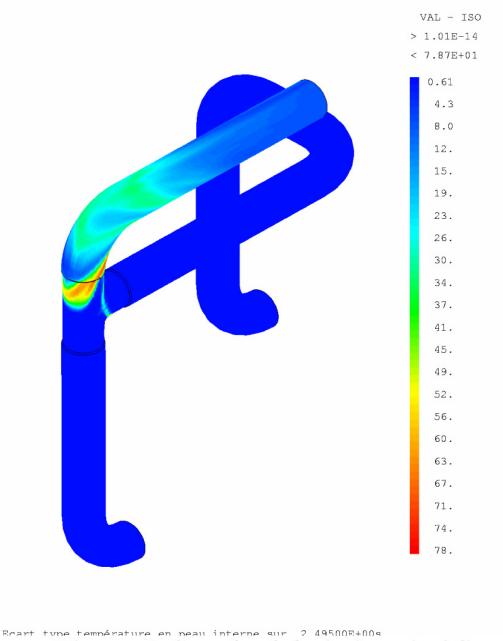

Figure 6: Standard deviations in °C

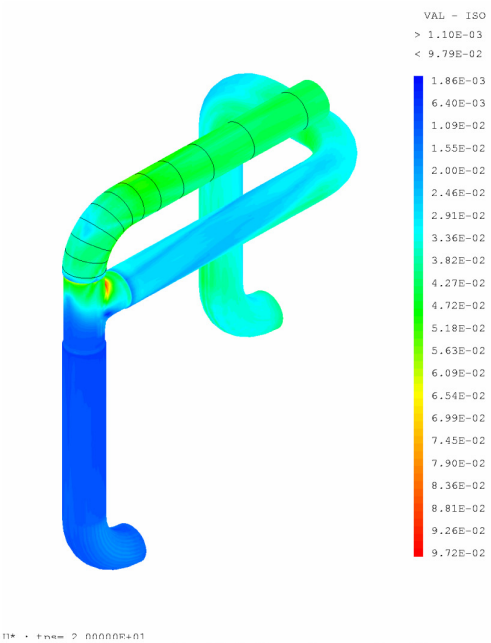

Figure 7: Friction iso-velocity

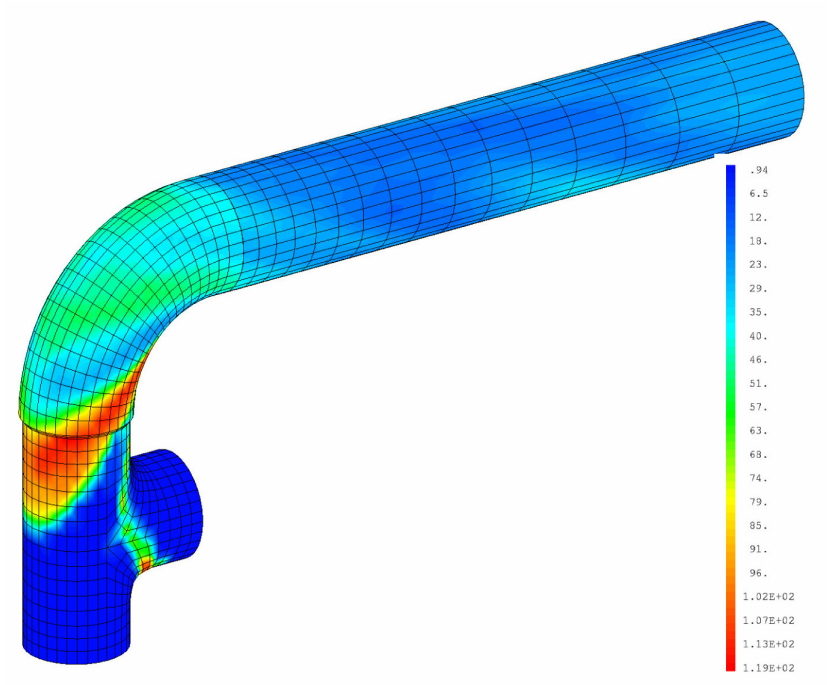

Figure 8: Temperature variation at the inner surface of the structure (°C)

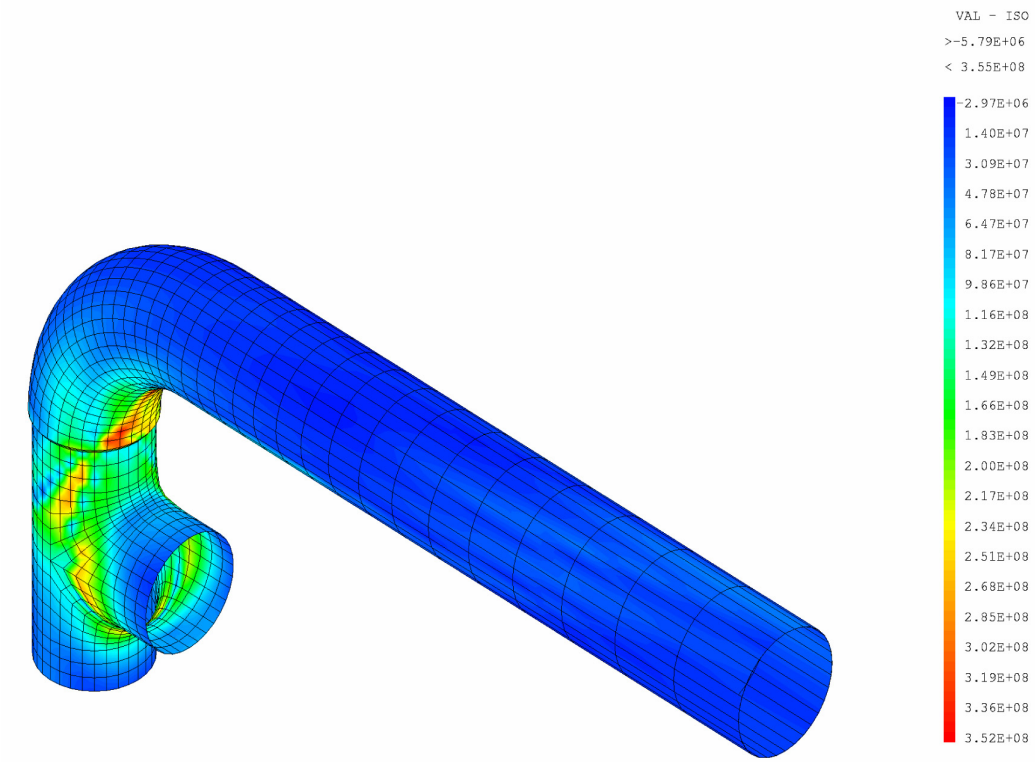

Figure 9: Average equivalent stress at the inner surface of the structure (MPa)

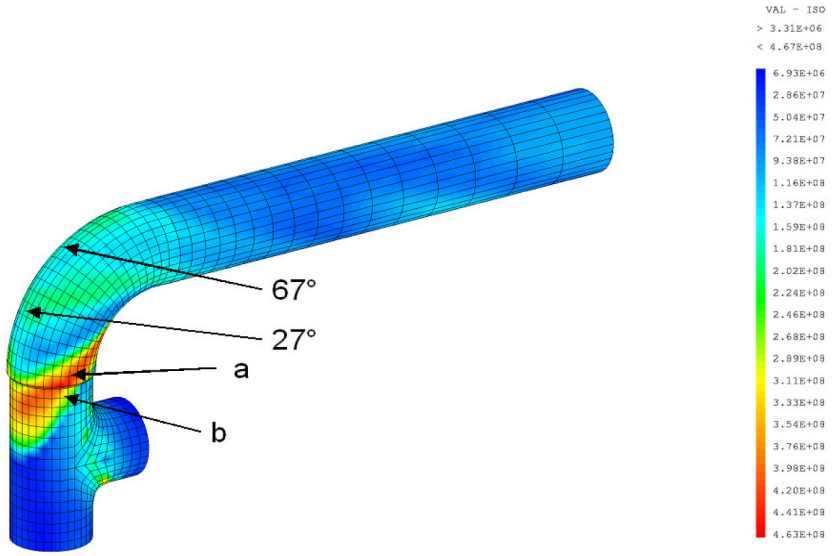

Figure 10: Equivalent stress variation at the inner surface of the structure (MPa)

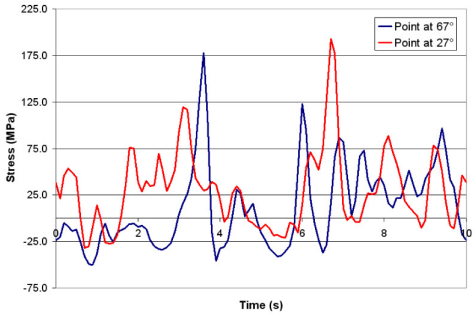

Figure 11: Stress variation in the elbow

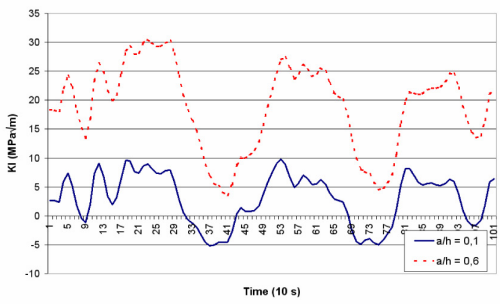

Figure 12: Variation of the stress intensity factor in the thin part of the tee

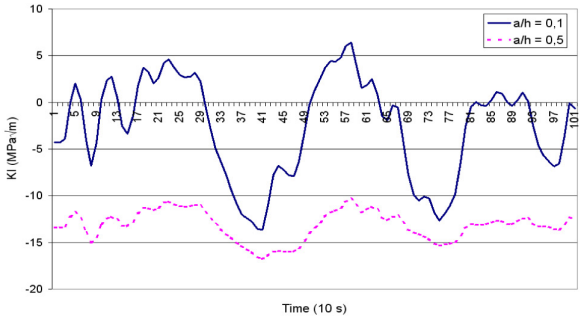

Figure 13: Variation of stress intensity in the thick part of the tee